LiDAR Map Construction Using Improved R-T-S Smoothing Assisted Extended Kalman Filter

Bo Zhang[1], Meng Wang[2], Shuhui Bi[1(✉)], and Fukun Li[1]

[1] School of Electrical Engineering, University of Jinan, Jinan 250022, China
cse_bish@ujn.edu.cn

[2] HRG Leapfound Robot Technology (Beijing) Co., Ltd., Beijing, China
wangmeng@hitrobotgroup.com

Abstract. On account of the low accuracy of boundary point cloud information during map construction of LiDAR used in mobile robots, an data processing scheme based on extended Kalman filter (EKF) and improved R-T-S smoothing and averaging is proposed to obtain accurate point cloud information. The proposed scheme can remove some noise points and make the map boundary more smoother and more accurate. The experimental results show that comparying with the original data, the proposed data processing scheme could reduce the position error of point cloud information effectively.

Keywords: LiDAR · Extended Kalman filter · R-T-S smoothing

1 Introduction

With the continuous improvement of the industrial level, the demand for robots in all walks of life is increasing day by day. A lot of work needs to be done indoors, and when mobile robots are used indoors, constructing accurate environmental information and precise positioning for mobile robots are the main points of autonomous navigation for robots [1–3].

The mobile robot's automatic path planning and automatic obstacle avoidance functions allow the mobile robot to travel safely in an unknown environment, which is inseparable from various sensors, examples include UWB [4], IMU [5], Camera and LiDAR [6]. Among them, the automatic obstacle avoidance technology mainly relies on drawing a point cloud through LiDAR to determine whether there are obstacles in front of the mobile robot [7]. Therefore, the accuracy of the point cloud diagram drawn by the LiDAR is the main factor affecting the automatic obstacle avoidance function.

Kalman filter(KF) is a highly efficient autoregressive filter, which can estimate the system state and reduce noise at the next moment based on the current system state [8,9]. However, the KF must be applied to a linear system conforming to the Gaussian distribution, so when targeting a nonlinear system, an EKF

W. Fu et al. (Eds.): ICMTEL 2021, LNICST 387, pp. 510–517, 2021.
https://doi.org/10.1007/978-3-030-82562-1_50

is required. The EKF is mainly to linearize the nonlinear system through Taylor expansion, and then perform the KF [10,11].

This paper proposes a scheme to process data by using a combination of EKF and R-T-S smoothing to overcome the shortcomings of large errors in a single sensor. The LiDAR data after EKF is then subjected to extended Kalman smoothing. The experimental results verify the effectiveness of this scheme. The rest of the paper is structured as follows: Sect. 2 establishes the motion model and studies the algorithm, Sect. 3 studies the performance of the proposed combined data processing scheme, and Sect. 4 gives the conclusion.

2 Map Construction Based on Extended Kalman Filter and Improved R-T-S Smoothing

The system flow chart is shown in Fig. 1. LiDAR obtains the point cloud information of the surrounding environment and establishes the state equation and observation equation. The data is input into the EKF, and the processed data is obtained through the processing of the EKF. Then input the EKF processed data into improved R-T-S smoothing to smooth the data. Finally, the average value of the improved R-T-S smoothing data is taken to obtain more accurate data.

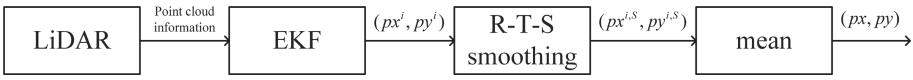

Fig. 1. System flow chart.

2.1 The LiDAR-Based Map Construction Model

The system is composed of LiDAR and observation target is shown in Fig. 2. The LiDAR is located at the origin of the coordinate system, and the observation target is point $P_k(px_k, py_k)$. At the moment k, dis_k is the distance between the LiDAR and the observation point P_k, and φ_k is the angle between the observation point and the X-axis. Then at the moment $k+1$, dis_{k+1} is the distance between the LiDAR and the observation point $P_{k+1}(px_{k+1}, py_{k+1})$, and φ_{k+1} is the angle between the observation point and the X-axis.

Use kinematics equations to describe the state equations of the points in the point cloud graph established by LiDAR is Eqs. 1 and 2. px_k is the position in the north direction, py_k is the position in the east direction, pV_k is the speed, φ_k is the heading angle, dt is the LiDAR obtains the time interval of two adjacent point clouds, ω_k is the system noise at time k and its covariance matrix is Q.

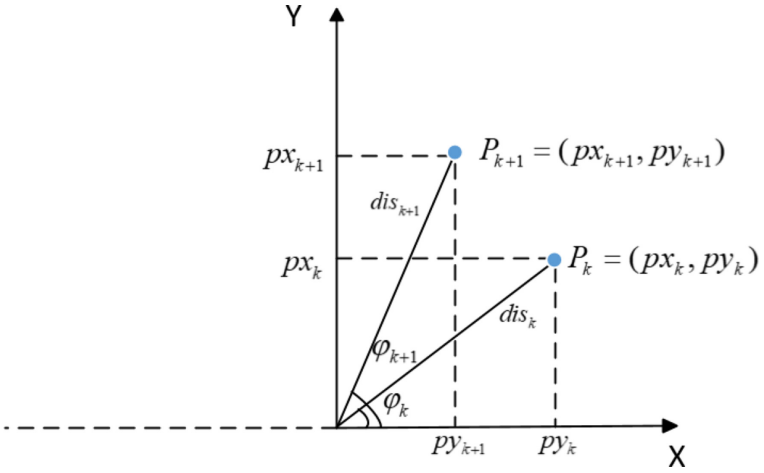

Fig. 2. Dynamic system model.

$$\underbrace{\begin{bmatrix} px_k \\ py_k \\ pV_k \\ \varphi_k \end{bmatrix}}_{\boldsymbol{X}_k} = \underbrace{\begin{bmatrix} px_{k-1} + dt \cdot pV_{k-1} \sin(\varphi_{k-1}) \\ py_{k-1} + dt \cdot pV_{k-1} \cos(\varphi_{k-1}) \\ pV_{k-1} \\ \varphi_{k-1} \end{bmatrix}}_{\boldsymbol{f}(\boldsymbol{X}_{k-1})} + \omega_k \tag{1}$$

Observation equations is listed as Eq. 3. h is the mapping of the landmark in the coordinate system, $dis_{j,k}$, $j = 1, 2, ..., i$ is the distance from LiDAR cloud point at time k to landmark j,$(lx^{(j)}, ly^{(j)}), j = 1, 2, ..., i$ is the position of the observation point, and j is the number of landmark. ν_k is the measurement noise.

$$\underbrace{\begin{bmatrix} dis_{1,k} \\ dis_{2,k} \\ \vdots \\ dis_{i,k} \end{bmatrix}}_{\boldsymbol{Z}_k} = \underbrace{\begin{bmatrix} \sqrt{(px_k - lx^{(1)})^2 + (py_k - ly^{(1)})^2} \\ \sqrt{(px_k - lx^{(2)})^2 + (py_k - ly^{(2)})^2} \\ \vdots \\ \sqrt{(px_k - lx^{(i)})^2 + (py_k - ly^{(i)})^2} \end{bmatrix}}_{\boldsymbol{h}(\boldsymbol{X}_{k-1})} + \nu_k \tag{2}$$

2.2 Principle of Extended Kalman Filter and R-T-S Smoothing

EKF is linearized on the basis of KF. Starting from the initial time, forward recursively at k time, then recursively from k time forward k times and backward recursive to complete the R-T-S smoothing process. Forward recursion is the EKF process(Eqs. 3 to 9), and backward recursion is the R-T-S smoothing process(Eqs. 9 to 3).

State Prediction

$$\hat{\boldsymbol{X}}_{k|k-1} = \boldsymbol{f}\left(\hat{\boldsymbol{X}}_{k-1}\right) + \omega_k \tag{3}$$

Among them: $\hat{\boldsymbol{X}}_{k|k-1}$ is the predicted value of the system state at time k at $k-1$, $\hat{\boldsymbol{X}}_{k-1}$ is the optimal estimation of the system state at $k-1$, ω_k is the amount of control given by the system.

Covariance Matrix Update

$$\boldsymbol{P}_{k|k-1} = \boldsymbol{A}_k\ \boldsymbol{P}_{k-1}\ \boldsymbol{A}_k^T + \boldsymbol{Q} \tag{4}$$

$$\boldsymbol{A}_k = \frac{\partial \boldsymbol{f}(\boldsymbol{X}_k)}{\partial \boldsymbol{X}_k} \tag{5}$$

Among them: $\boldsymbol{P}_{k|k-1}$ is the covariance matrix corresponding to the state $\hat{\boldsymbol{X}}_{k|k-1}$ to be calculated, $\boldsymbol{A}_k$ is the partial derivative Jacobian matrix of $\boldsymbol{f}$, and $\boldsymbol{P}_{k-1}$ is The calculated covariance matrix of $\hat{\boldsymbol{X}}_{k-1}$, $\boldsymbol{Q}$ is the covariance matrix of system process noise

Calculate Weight

$$\boldsymbol{K}_k = \ \boldsymbol{P}_{k|k-1}\ \boldsymbol{H}_k^T \left(\boldsymbol{H}_k\ \boldsymbol{P}_{k|k-1}\ \boldsymbol{H}_k^T + \boldsymbol{R}_k\right)^{-1} \tag{6}$$

$$\boldsymbol{H}_k = \frac{\partial \boldsymbol{h}(\boldsymbol{X}_k)}{\partial \boldsymbol{X}_k} \tag{7}$$

Among them: $\boldsymbol{R}_k$ is the covariance matrix of the system observation noise, $\boldsymbol{H}_k$ is the $\boldsymbol{h}$ partial derivative Jacobian matrix obtained in the previous part, $\boldsymbol{K}_k$ is the Kalman gain, based on the covariance matrix of the system's predicted state and sensor observations, to determine the weight ratio of each in the posterior probability.

Estimate Current State

$$\hat{\boldsymbol{X}}_k = \hat{\boldsymbol{X}}_{k|k-1} + \boldsymbol{K}_k \left(\boldsymbol{Z}_k - \boldsymbol{h}(\hat{\boldsymbol{X}}_{k|k-1})\right) \tag{8}$$

Combine the predicted value $\hat{\boldsymbol{X}}_{k|k-1}$ in the first step and the observation value $\boldsymbol{Z}_k$ of the sensor at the current moment, take the $\boldsymbol{K}_k$ calculated in the third step as the weight, and calculate the weighted sum of the current moment The best estimate $\hat{\boldsymbol{X}}_k$.

Update Covariance

$$\boldsymbol{P}_k = (\boldsymbol{I} - \boldsymbol{K}_k \boldsymbol{H}_k)\, \boldsymbol{P}_{k|k-1} \tag{9}$$

The update of the covariance can not only ensure the accuracy of the covariance at the next moment, but more importantly, because the prior estimate at the next moment comes from the posterior estimate at the previous moment, the algorithm can iterate continuously to achieve self return.

3 Experiment and Discussion

3.1 Experiment Environment

Article conducted an experiment in University of Jinan to verifies the effectiveness of the scheme. The experiment consists of a portable computer, LiDAR and a support. The portable computer and LiDAR are connected by micro USB and USB to serial port module. LiDAR is responsible for collecting the point cloud information of the surrounding environment, and the portable computer is mainly responsible for saving the LiDAR point cloud data and processing the EKF algorithm. LiDAR is located on the support. The schematic diagram is shown in Fig. 3.

The reference position, the LiDAR data and the position after EKF and improved R-T-S smoothing are shows in Fig. 4. In this figure, we can see that the point cloud information after EKF and improved R-T-S smoothing is more accurate than before.

Fig. 3. Test environment.

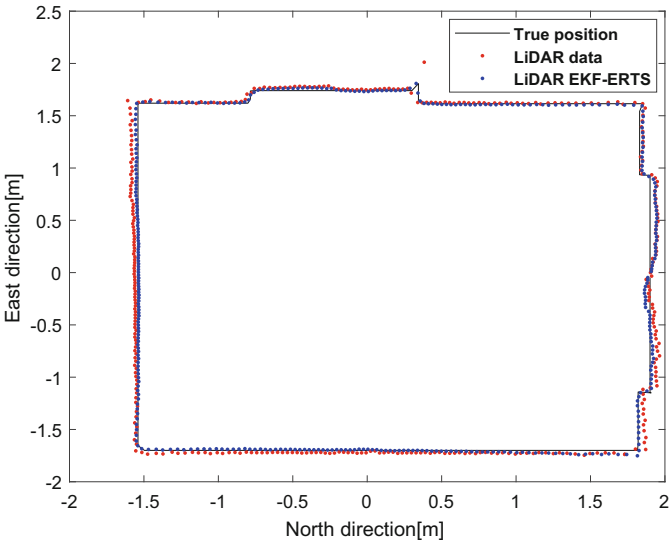

Fig. 4. The reference position, the LiDAR data and the position after EKF and improved R-T-S smoothing.

3.2 Performance of the Scheme

The RMSE calculation is performed on the point cloud data collected by LiDAR and the point cloud data calculated by the EKF, and the results are shown in Table 1. In this table, the data processed by EKF and improved R-T-S smoothing obviously has smaller error than before processing. The root mean square error(RMSE) after EKF and improved R-T-S smoothing of position in north is 0.0166 m and in east is 0.0164 m.

Table 1. RMSE(m) in two directions.

Direction	Before extended Kalman filter	After extended Kalman filtering
East direction	0.0242	0.0164
North direction	0.0247	0.0166
Mean	0.02445	0.0165

The position error in north direction and east direction is shown in Figs. 5 and 6.

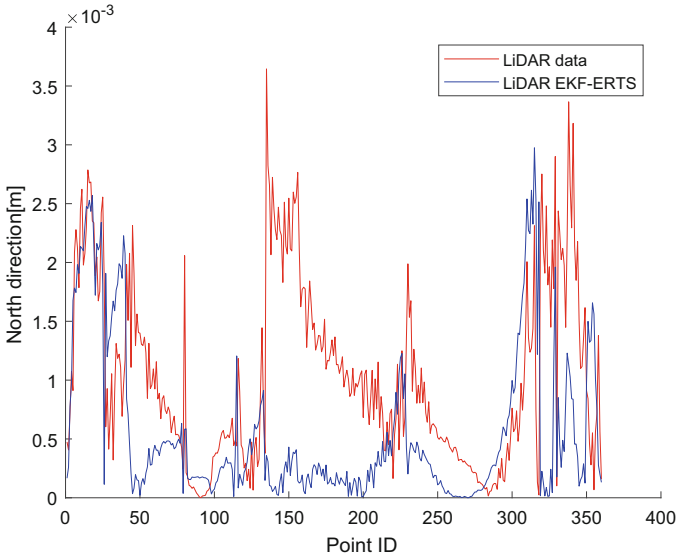

Fig. 5. Position error in north direction.

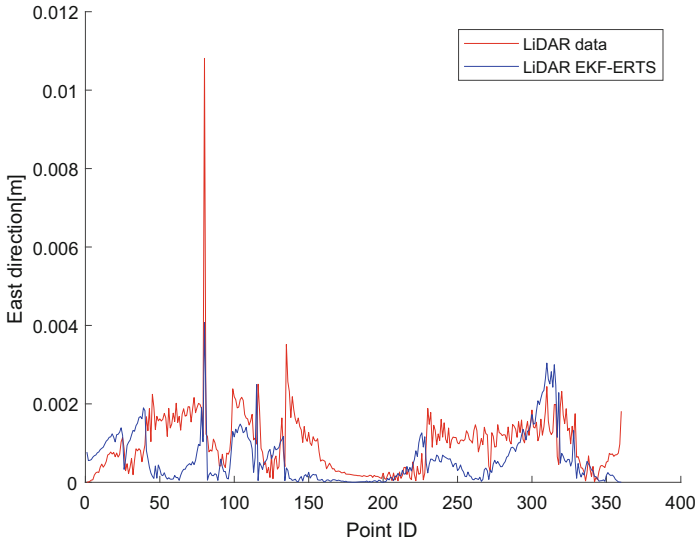

Fig. 6. Position error in east direction.

4 Conclusions

A LiDAR point cloud information graph processing method based on EKF and improved R-T-S smoothing is proposed. In this scheme, the LiDAR point cloud

information is processed by using EKF and then the filtered data is smoothed by improved R-T-S smoothing. The experiment verifies the effectiveness of EKF and improved R-T-S smoothing in reducing the position error relative to the original data.

Acknowledgment. This paper was supported by National Natural Science Foundation of China (No. 61803175), Shandong Provincial Natural Science Foundation (No. ZR2018LF01, No. ZR2020KF027), Shandong K&D Program (No. 2019GGX104026).

References

1. Sherwin, T., Easte, M., Chen, A.T., et al.: Robocentric map joining: improving the consistency of EKF-SLAM. Rob. Auton. Syst. **55**(1), 21–29 (2007)
2. Xu, Y., Shmaliy, Y.S., Li, Y., et al.: UWB-based indoor human localization with time-delayed data using EFIR filtering. IEEE Access **5**, 16676–16683 (2017)
3. Song, J., Zhang, W., Wu, X., et al.: Laser-based SLAM automatic parallel parking path planning and tracking for passenger vehicle. IET Intell. Transp. Syst. **13**(10), 1557–1568 (2019)
4. Xu, Y., Ahn, C.K., Shmaliy, Y.S., et al.: Adaptive robust INS/UWB-integrated human tracking using UFIR filter bank. Measurement **123**, 1–7 (2018)
5. Xu, Y., Ahn, C.K., Shmaliy, Y.S., et al.: Tightly-coupled integration of INS and UWB using fixed-lag extended UFIR smoothing for quadrotor localization. IEEE Internet Things J. **8**(3), 1716–1727 (2018)
6. Hutabarat, D., Rivai, M., Purwanto, D., et al.: LiDAR-based obstacle avoidance for the autonomous mobile robot. In: 2019 12th International Conference on Information and Communication Technology and System (ICTS), pp. 197–202. Surabaya (2019)
7. Chelghoum, A., Wang, Q., Wang, K.: Design and simulation of autonomous mobile robots obstacle avoidance system. In: Pan, Z., Cheok, A.D., Müller, W., Zhang, M. (eds.) Transactions on Edutainment XIII. LNCS, vol. 10092, pp. 165–180. Springer, Heidelberg (2017). https://doi.org/10.1007/978-3-662-54395-5_15
8. Zhao, S., Huang, B.: Trial-and-error or avoiding a guess? Initialization of the Kalman filter. Automatica **121**, 109184 (2020)
9. Zhao, S., Shmaliy, Y.S., Liu, F.: Fast Kalman-like optimal unbiased FIR filtering with applications. IEEE Trans. Sig. Process. **64**(9), 2284–2297 (2016)
10. Pengfei, S., Lilan, L., Zenggui, G., et al.: On the target tracking and locating method using EKF algorithm in service robots. Metrol. Meas. Tech. **46**(1), 1–4 (2019)
11. Li, X., Wang, Y., Liu, D.: Research on extended Kalman Filter and particle filter combinational algorithm in UWB and foot-mounted IMU fusion positioning. Mob. Inf. Syst. **4**, 1–17 (2018)